Journal of Engineering Science and Technology
Vol. 16, No. 1 (2021) 365 - 384

LOW VOLTAGE RIDE THROUGH CAPABILITY ENHANCEMENT USING SERIES CONNECTED FACT DEVICES IN WIND ENERGY CONVERSION SYSTEM

BIBHU PRASAD GANTHIA*, SUBRAT KUMAR BARIK, BYAMAKESH NAYAK

School of Electrical Engineering, Kalinga Institute of Industrial Technology (KIIT),Deemed to be University, Bhubaneswar, Odisha, India
*Corresponding Author: jb.bibhu@gmail.com

Abstract

The complete assessment of the various strategies used to decorate the skills of Low Voltage Ride Through (LVRT) of Double Fed Induction Generators (DFIG) primarily based Type-III wind turbine systems (WT) explained in this research paper. In this paper, simulation results in MATLAB show that a DFIG based Type-III wind turbine system do not have the LVRT capacity due to insufficient reactive power support during disturbances using conventional PI controller. Hence using proposed Mode 4 Type-I fuzzy logic controller in associated with series connected FACTS devices can improve the LVRT capacity of DFIG based WECS, with DVR providing better VAR compensating capacity than other series connected FACTs devices. Type-III wind turbine system with DFIG based WECS has better LVRT capacity and voltage stability due to its real and reactive power control ability using proposed controller technique. Therefore, unique LVRT approaches based at the implementing additional active interface technologies had been proposed in this paper. Many techniques are developed nowadays to overcome the issue of this low voltage due to faults. This paper tries to define such active methods to short the gap by presenting a complete analysis of these LVRT strategies for DFIG based WECS in terms of overall adaptive performance, complexity of controllers, and cost effectiveness using fuzzy logic controller. Here characteristic of this paper is to highlight the methods for increasing the ability of LVRT relying on the configuration of the relationship into 3 major areas according to its grid integrations. In this paper smooth and simple series connection of FACT devices are used in WECS to study its effectiveness and benefits. The mathematical models of the whole system are simulated through MATLAB Simulink and results are discussed. In this paper all the types of wind turbine systems (Type-I and Type-II) are implemented by FACT devices with comparison to previous works and the faster FACT device is used on new proposed Type-III wind turbine system with fully control mechanisms (aerodynamic, mechanical, electrical and drive train system) are introduced to get more stability in the power system operation and control.

Keywords: DFIG, FACTs, FSIG, LVRT, Type-I FLC, Type-III WT, WECS.

1. Introduction

The objective of this paper is decreasing ozone depleting substance discharges is the vital issue which related with the development and entrance of sustainable power sources [1, 2]. Introduced wind turbines (WTs) are focused on power system stability using grid integrations to enhance the power quality during faults. However, grid integration into the wind energy system of large WTs can cause serious side effects in poor or weak grids. The inclination towards more WT integration is to build the present degree of the unbalancing just as decline the voltage over the wind generators system, which can prompt the fault clearances of the WT. As of late, many power system techniques are in everywhere throughout the world have started to grow and alter their correspondence prerequisites for wind cultivates by specialized models, known as grid codes which is one of the significant necessities with respect to grid voltage control is the capacity of the Low Voltage Ride Through (LVRT), which is remembered for a few new grid codes. Figure 1 delineates the LVRT bend in activity for grid associated WTs [3].

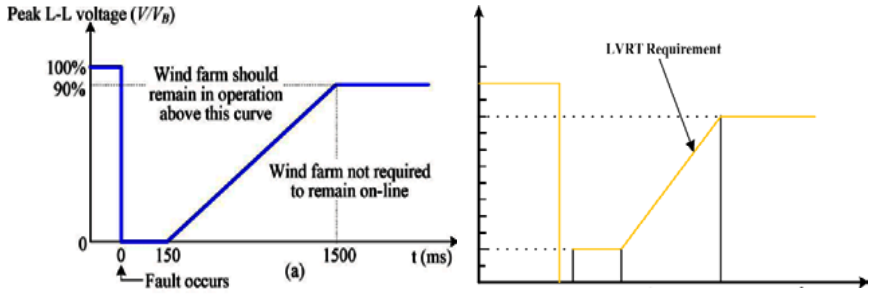

Fig.1. LVRT curve.

Depending on this principle, the WT must be connected to the grid if the voltage stays at a level more than 20 m/s than the nominal value for length less than 0.5 m/s [4]. WTs can be disconnected from the grid only on instance of voltage profile dropped in region B, close to the LVRT requirements where grid codes additionally need huge WTs to reply throughout error and retrieval. Inject strength of the machine to contribute to the protection of the voltage of the energy devices. The blue line and the orange line signify the LVRT requirement line of grid code which defines the voltage sag condition during the grid unbalance and voltage swell conditions during transients due to rapid variations in wind speeds [5, 6]. This LVRT curve represents the operating regions during normal and abnormal condition of the wind speed.

The literature reviews on the recent research hybrid FACTs devices are implemented for the LVRT capability enhancements using adaptive control techniques [2-7, 9-12]. Comparing with the hybrid; series compensating techniques can show faster steady state and reactive power compensations using adaptive techniques for the controlling the error in the system gains[13, 14]. Previously connectional PI controllers are used for the transient analysis [15, 16, 18]. Then it switches over to the adaptive techniques like genetic algorithm based and other meta heuristic techniques [17, 19, 20]. These techniques are very complex and needs more optimizations [20]. Hence in this paper Mode-4-Type-I fuzzy logic

controller is implemented to get faster response during the transients due to sudden change in wind speeds [2-5].

2. Wind Energy Conversion System

There are three forms of machines utilized in wind energy conversion structures which can be stated in preceding section. The model of WECS contains three key differentiators, they are aerodynamic core, mechanical system and electrical as shown in Fig. 2. In the electrical component of WECS can similarly be divided into three main component systems, which can be utility grid, power electronics converters (PECs) and wind turbine generators (WTGs) [1, 2].

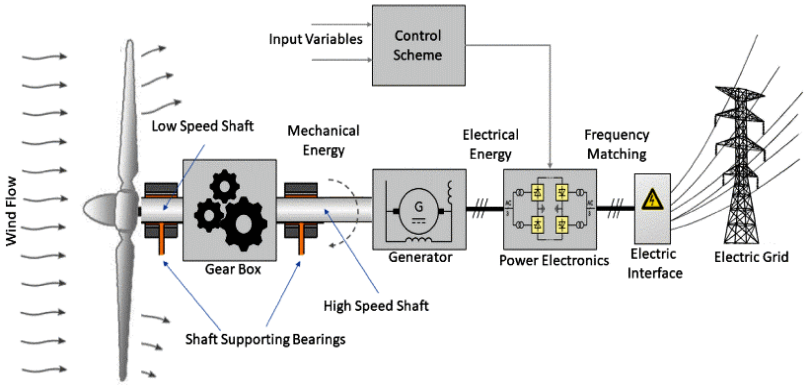

Fig.2. Wind energy conversion system.

The captured aerodynamic power shown below in Eq.(1) calculates for the wind turbine is given by:

$$P_{wt} = ½ \rho\pi R^2 V^3 \quad (1)$$

where, ρ defines the air density [kg/m^3], V shows the wind speed [m/s], R is the blade radius [m], Pwt is the power. The mechanical power for the turbine can extract maximum power depends on power coefficient Cp can be given in Eq.(2) shown below:

$$P_{mec} = C_p P_{wt} = ½ C_p \rho\pi R^2 V^3 \quad (2)$$

From Eqs. (1) and (2) it is obvious that the energy generated increases with blade area, wind speed, air density and power coefficient.

3. Double Fed Induction Generator

The recent study on wind turbine with DFIG is used where back-to-back voltage source converter feeds the rotor winding. A gearbox is vital to couple the rotor to the generator just like the preceding case, because of the difference within the rotor and generator pace stages. The mathematical modelling of wind turbine system using DFIG is used as it can be fully controlled during variations in wind speed. The mechanical drive train system can be associated with the electrical system to make this system fully control [3, 4].

The stator winding of the DFIG is coupled to the network, the rotor winding is coupled to rotor side converter (RSC) and the scientific notations appeared in Fig. 3. Then the rear side of consecutive voltage source converter specifically grid side converter (GSC) that takes care of the rotor winding is coupled to the grid network. A DC link is connected to decoupled frame of RSC and GSC [2].

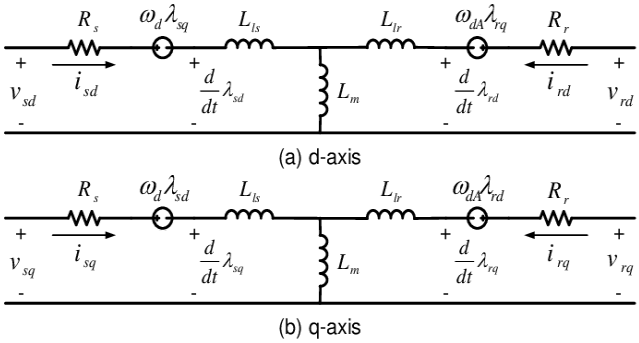

Fig.3. Wind energy conversion system.

4. Type-III Wind Turbine Electrical Model

Type I DFIG system is based on fixed speed rather a Type II DFIG wind system is operated under partial variable speeds. In Type III DFIG system it can work under variable wind speed in partial scale control action shown in Fig. 4. The Type IV DFIG system is variable speed of operation in full scale controller. The Type-III DFIG equations according to axis d and q scheme can be expressed as [2, 3].

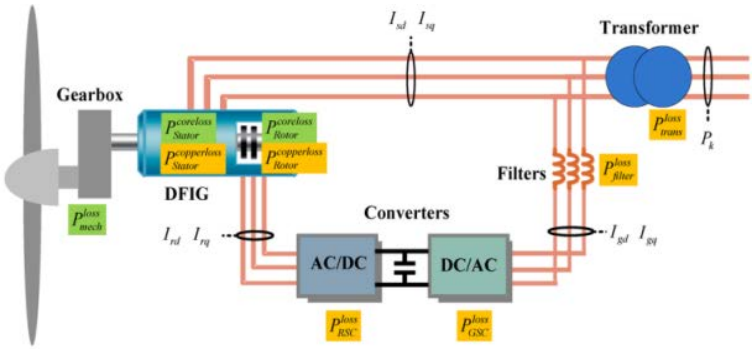

Fig.4. Type III DFIG-based wind generator.

The model shown in the Fig. 4 depicts the control action of Type-III DFIG under the transients and the rotor side, grid side control operations using the stator voltage control mechanism. The control is also using a conventional PI controller of control system for the steady state and transient actions of settling time during fault clearances [3].

$$v_{ds} = -R_s x i_{ds} + (x_s + x_m)\, x\, i_{qs} + x_m x i_{qr} \quad (3)$$

$$v_{qs} = -R_s x i_{qs} - (x_s + x_m) x i_{ds} + x_m x i_{dr} \quad (4)$$

$$v_{dr} = -R_r x i_{dr} + (1-\omega) x ((x_r + x_m) x i_{qr} + x_m x i_{qs} \quad (5)$$

$$v_{qr} = -R_r x i_{qr} + (1-\omega) x ((x_r + x_m) x i_{dr} + x_m x i_{ds} \quad (6)$$

where: *vds*, *vqs* are d and q axes of the stator voltages; *vdr*, *vqr*, d and q axes of the rotor voltages; *ids*, *iqs*, d and q axes of the stator currents; *idr*, *iqr*, d and q axes of the rotor currents; *Ra*, *Rr*, stator and rotor resistance; *xs*, stator self-reaction; *xr*, rotor self-reaction; *xm*, rotor speed. The inserted active and reactive forces in the network can be expressed as given below [2, 3]:

$$P = v_{ds} x i_{ds} + v_{qs} x i_{qs} + v_{dr} x i_{dr} + v_{qr} x i_{qr} \quad (7)$$

$$Q = -\frac{x_m v i_{dr}}{x_s + x_m} - \frac{v^2}{x_m} \quad (8)$$

Here v is the magnitude of grid voltage.

The Type-III DFIG has the mechanical motion system associated with the wind gear box and coupled to the blades [3, 4].The motion equation of the wind turbine system derives the torque due to electromagnetic effect and the mechanical torque. The equations are shown as follows:

$$\left.\begin{aligned} J\frac{dw_m}{dt} &= T_e - T_m \\ T_e &= \frac{3P}{2} Re(j\vec{\lambda}_s \vec{i}_s^{\,*}) = -\frac{3P}{2} Re(j\vec{\lambda}_s \vec{i}_r^{\,*}) \end{aligned}\right\} \quad (9)$$

where Here *J* = MI-moment of inertial of the rotor (kgm^2), *P* = number of poles, *Tm* = Mechanical Torque (N.m), *Te* = Electromagnetic Torque (N.m), and *wm* = Rotor Mechanical Speed (rad/s)

The mathematical modeling of Type-III base on dq frame of reference conversion in dq axis representations. The modeling equations are present below:

$$\begin{aligned} \overrightarrow{v_s} &= v_{ds} + jv_{qs} \\ \overrightarrow{v_r} &= v_{dr} + jv_{qr} \end{aligned} \quad (10)$$

$$\begin{aligned} \vec{i}_s &= i_{ds} + ji_{qs} \\ \vec{i}_r &= i_{dr} + ji_{qr} \end{aligned} \quad (11)$$

$$\begin{aligned} \vec{\lambda}_s &= \lambda_{ds} + j\lambda_{qs} \\ \vec{\lambda}_r &= \lambda_{dr} + j\lambda_{qr} \end{aligned} \quad (12)$$

Voltage equations for stator and rotor in dq axis frame are:

$$\begin{cases} v_{ds} = R_s i_{ds} + p\lambda_{ds} - w\lambda_{qs} \\ v_{qs} = R_s i_{qs} + p\lambda_{qs} + w\lambda_{ds} \\ v_{dr} = R_r i_{dr} + p\lambda_{dr} - (w - w_r)\lambda_{qr} \\ v_{qr} = R_r i_{qr} + p\lambda_{qr} + (w - w_r)\lambda_{dr} \end{cases} \quad (13)$$

Flux linkages to stator and rotor in dq axis reference frame are:

$$\begin{cases} \lambda_{ds} = (L_{ls} + L_m) i_{ds} + L_m i_{dr} = L_s i_{ds} + L_m i_{dr} \\ \lambda_{qs} = (L_{ls} + L_m) i_{qs} + L_m i_{qr} = L_s i_{qs} + L_m i_{qr} \\ \lambda_{dr} = (L_{lr} + L_m) i_{dr} + L_m i_{ds} = L_r i_{dr} + L_m i_{ds} \\ \lambda_{qr} = (L_{lr} + L_m) i_{qr} + L_m i_{qs} = L_r i_{qr} + L_m i_{qs} \end{cases} \quad (14)$$

Motion due to mechanical rotation is shown in equations in dq reference frame are:

$$\begin{cases} T_e = \frac{3P}{2}(i_{qs}\lambda_{ds} - i_{ds}\lambda_{qs}) \\ T_e = \frac{3P}{2}(i_{qs}i_{qr} - i_{ds}i_{qr}) \\ T_e = \frac{3P}{2}(i_{qs}\lambda_{dr} - i_{ds}\lambda_{qr}) \end{cases} \quad (15)$$

5. Type-III Wind Turbine Mechanical Drive Train Model

The wind turbine mechanical torque can be presented as T_m is [1, 3, 4]:

$$T_m = \frac{p_w}{\omega} \quad (16)$$

The wind turbine system can extract the as *Pw* is:

$$p_w = \frac{1}{2}\rho c_p A * V_w^3 \quad (17)$$

where: c_p - power coefficient, ω - rotor speed, ρ - air density (kg/m^2), A - rotor area (m^2) and V_w (m/s) - wind velocity. Thus, the electrical torque T_e and the mathematical link between T_m and T_e results:

$$T_e = x_m(i_{qr}i_{ds} - i_{dr}i_{qs}) \quad (18)$$

$$\frac{d\omega}{dt} = \frac{1}{2H}(T_m - T_e) \quad (19)$$

Here H is denoting rotor inertia.

Mathematically wind speed V_w(t) is characterized by four components of its controls: i) Initial and average value of wind speed V_{wa} (m/s); ii) Ramp component V_{wr} (t); iii) The gust component V_{wg} (t) iv) Turbulence of wind speed V_{wt} (t). Therefore, the mathematically wind speed V_w(t) represented as follows:

$$V_w(t) = V_{wa} + V_{wr}(t) + V_{wg}(t) + V_{wt}(t) \quad (20)$$

Figure 5 represents the generation of wind speed in artificial manner through the Gaussian noise generator using ARMA (autoregressive moving average) technique taking unity delay function [4].

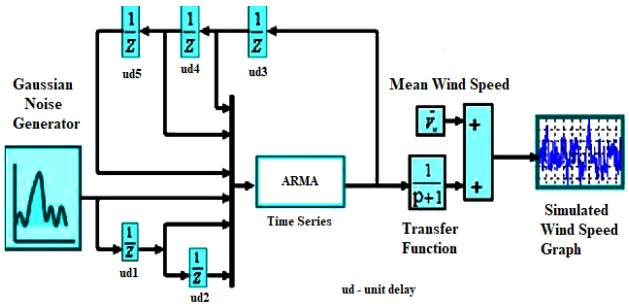

Fig.5. Typical configuration of ARMA wind speed model.

6. Mode 4 Type-I Fuzzy Logic Controller

Using conventional PI controller in the wind turbine system during grid integration it shows sluggish steady state and transient analysis [1]. Hence new adaptive techniques

are implemented for faster transient response during faults. Sugeno-Takagi Type-I fuzzy logic controller can use to enhance the stability during grid integration when faults arise due to sudden changes in wind speeds. This proposed technique Mode 4 Type-I FLC can incorporated with FACTs devices and conventional PI controller to enhance low voltage ride through capabilities and can control the reactive power. This reactive power can be use during sag and swell of voltage due to the transients. The propose technique controls both sag and swell with considering constraints of weather conditions [1, 2].

The proposed controller outputs during operation are more reliable and efficient because here the effect of unwanted aspects or parameters like noise, harmonics and cause due to range of wind speed control and the area are taken into consideration. Sugeno-Takagi Type-I fuzzy set model developed here shown in Figs. 6 and 7 and initiated to control the reactive power (Q) and stator active power (P) of the WECS.

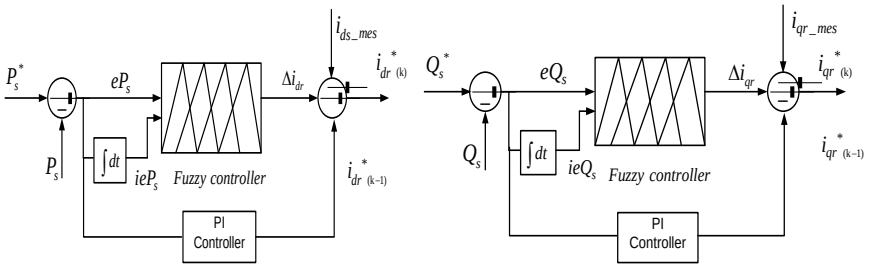

Fig.6. Control scheme of P and Q with error and integration of error as input with PI controller.

The membership function for active and reactive power input and output is given as:

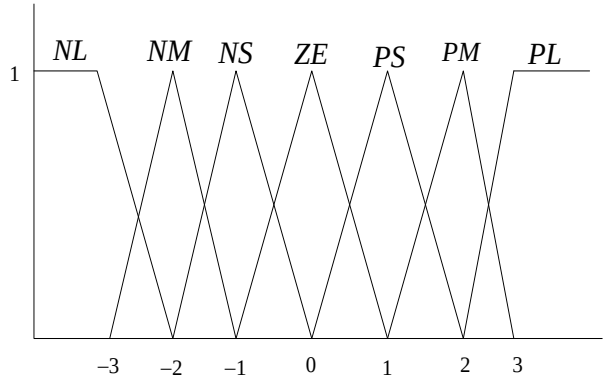

Fig.7. Triangular membership function for error, change in error, integration of error and output.

7. Low Voltage Ride Through Methods

The LVRT methodologies are classified into series, shunt and hybrid system associated with wind energy system. Some series connected flexible AC transmission system (FACTs) devices shown in Fig. 8 are: dynamic voltage restore (DVR), thyristor-controlled series compensation (TCSC), magnetic energy

recovery switch (MERS), series dynamic braking resistor (SDBR) and fault current limiter (FCL). In this paper three important series connected solutions are discussed and comparisons based on the implementations are also highlighted. A suitable series connected device taken which used during grid integration with proposed controller (Mode 4 Type-I FLC) [1].

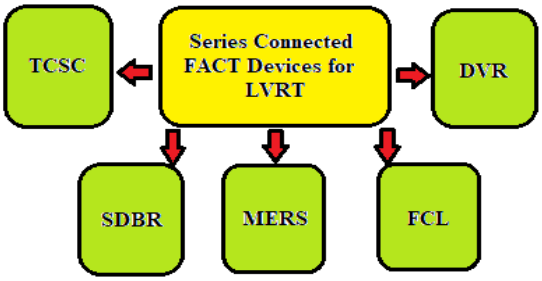

Fig.8. Classified LVRT capability enhancement methods.

8. FACT Devices in WECS

8.1. Thyristor controlled series compensation (TCSC)

The fundamental standard of the TCSC is to control power stream of the grid lines, increment the dynamic steadiness of intensity transmission and adequately limit the power transients [1].

Figure 9 shows a common TCSC module introduced surroundings of the wind system along the essential control mechanism. This FACT device (TCSC) comprises of three segments: bypass sidestep inductor L, capacitor banks C and forward biasing thyristors T1 and T2. In this control mechanism the operation on variation in voltage are reported in this paper. This innovation might be valuable for wind ranches situated a long way from the PCC, for example, offshore farms of wind system [5].

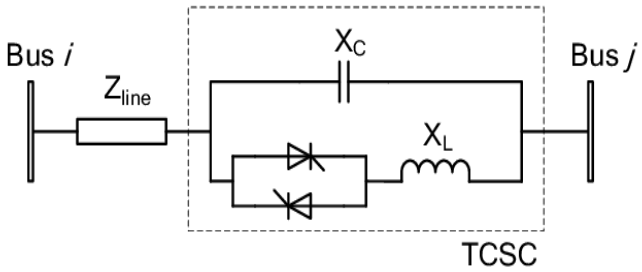

Fig.9. Circuit diagram of TCSC.

8.2. Dynamic voltage restorer (DVR)

Grid fault identified with WT generators is a promising way to deal with adequately to clear the issues and incrementing ride through capacity shown in Fig. 10. This should be possible utilizing power electronic chargers integrated with the system,

called dynamic voltage restorers (DVRs) which put a sensible voltage on the PCC and on the grid bus to keep up generator voltage [1, 6].

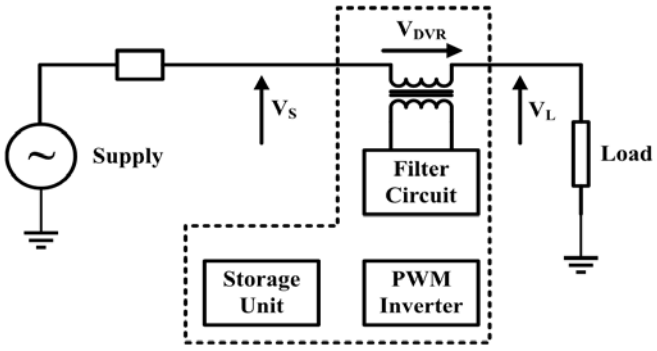

Fig.10. Circuit diagram of DVR.

8.3. Series dynamic braking resistor (SDBR)

SDBRs were developed to directly contribute to the equalization of active power between the mechanical and electrical side of the WT framework during the fault, conceivably diminish the requirement for reactive power compensation (RPC) and pitch angle control devices appeared in Fig. 11 [1].

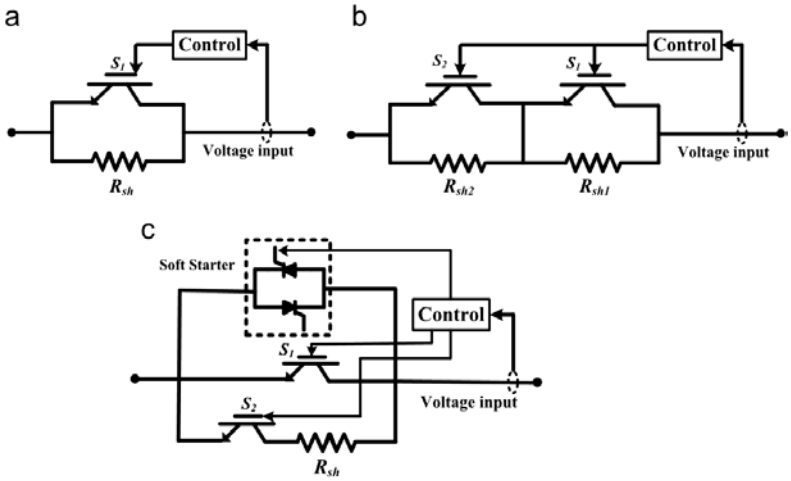

Fig.11.Types of SDBR (a) Stage 1 normal scheme (b) Stage 2 switching scheme (c) Stage 3 variable resistor scheme.

It is achieved through dynamically adding a series resistor between the WT and the grid to assist the voltage at the generator terminals, thus the reliability issues regarding electrical torque and power throughout the time frame of fault [1].

9. Steady State Analysis

The WT discharges power from the air through sharp edges fabricated by aerodyne and changes it into mechanical quality. In steady state analysis under high-

speedwind variations and power provided by WT can surpass its rated parameters. The aerodynamics of the accelerated wind turbines control and operated by uninvolved slow down, active slow down and pitch control mechanisms intended for low, medium, and enormous wind turbines [8].

10. Transient State Analysis

In transient analysis at the point when the fault happens at the WT terminals drops, hence lessening the power yield from the electromagnetic torque and induction generator. In any case, the mechanical information torque stays steady during the fault, which makes the rotor's speed surpass its well-being limit with the goal that greatest vitality can be put away precisely [1, 8].

11. MATLAB Simulink Model

The models are designed using MATLAB Simulink. The system is associated with the PI controller and adaptive Mode 4 Type-I fuzzy logic controller for the steady state and transient analysis the settling time after fault clearance also reported from the simulations. The systems are discussed with all three FACT devices implemented with the wind energy conversion modelling.

The Simulink diagram Fig. 12 shows the TCSC action in reactive power control during faults. Figure 13 associateswith the DVR action and Fig. 14 highlights the action using SDBR device connected in series with the system.

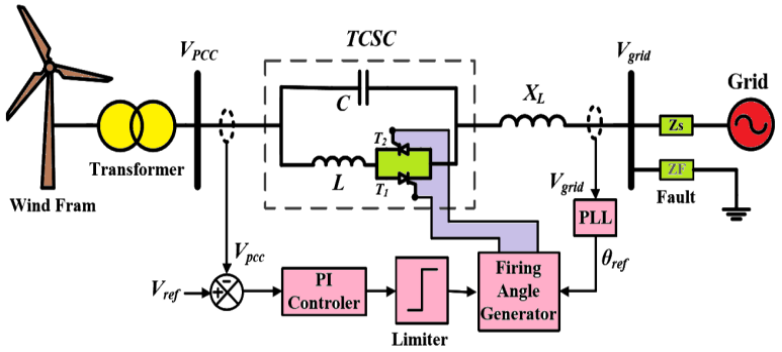

Fig.12. TCSC module installed in wind turbine.

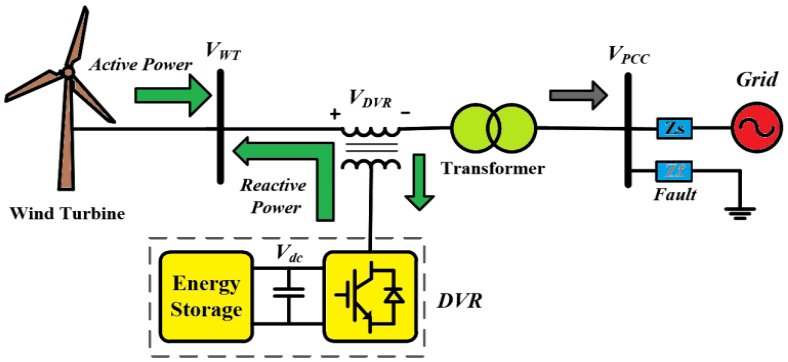

Fig.13. Dynamic voltage restorer with wind turbine.

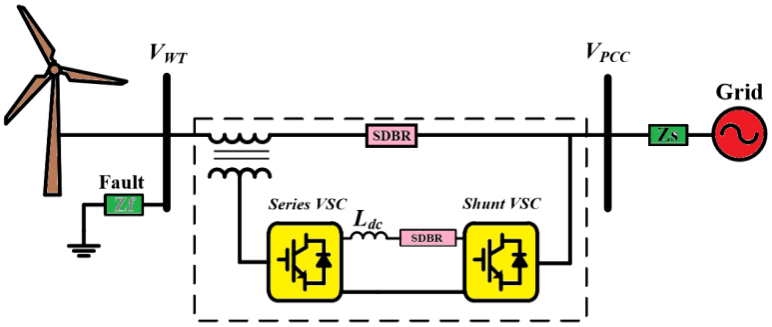

Fig.14. Wind turbine with SDBR.

12. Simulink Results, Performances Comparison and Discussion

Figure15 shows the simulation results of the DFIG system under grid voltage unbalance fault (a) stator grid voltage(W), (b) electromagnetic torque (W), (c) stator flux (W), (d) active & reactive power, (e) stator current, (f) rotor current, (g) modulated voltage, (h) DC-link voltage.

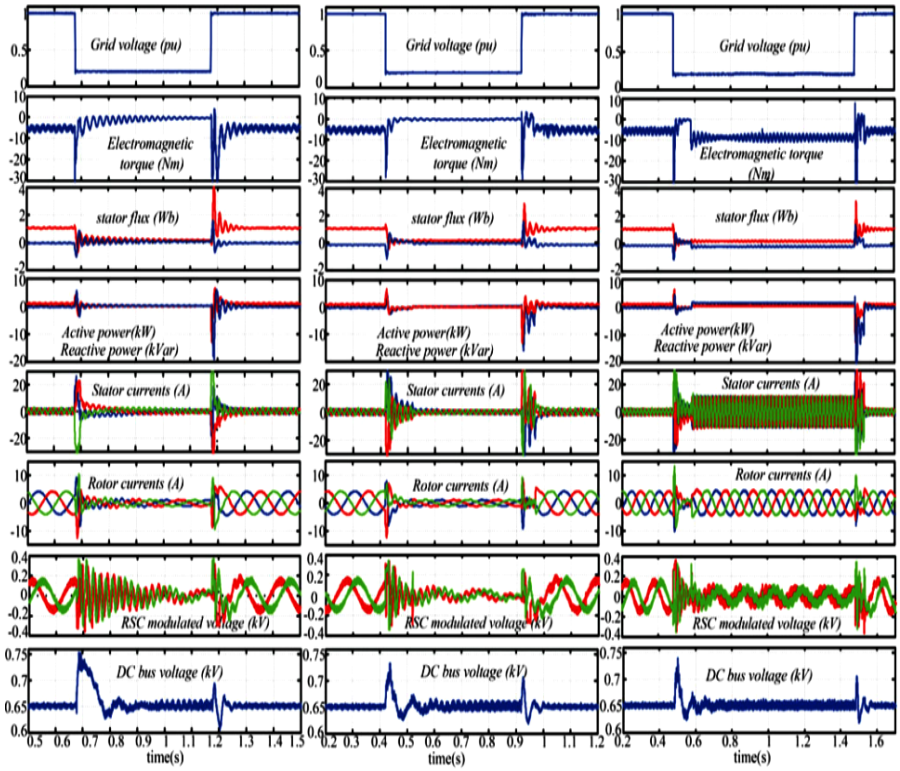

(a)TCSC **(b)DVR** **(c)SDBR**

Fig.15. DFIG transient analysis using TCSC, DVR and SDBR.

The above Simulink results have shown in Fig. 15 highlights the control action of FACT devices as given in the design model to control the reactive power during low voltage transient analysis. Here both steady state and transient analysis are done to know both the virtual and direct effects of low voltages due to the unwanted faults. From the above Simulink result it is clearly indicating the control actions during the faults during 0.4 sec to 0.9 sec the wind turbine parameters are changes. In case of DVR shown in Fig. 15,Section B highlights the transient time duration of 0.4 sec to 0.9 sec, it clears the fault before the 1sec rather in Section A it is 1.2 sec and in Section C it is found that about 1.5sec. With comparison to other flexible ASC transmission devices as controller DVR shows faster response among series connected devices. Hence it can be used further with the proposed control technique (Mode 4 Type-I fuzzy logic) to control the reactive power to achieve faster steady state and remove transients due to sudden change in wind speeds.

The Simulink model shown in Fig. 16 below depicts the control model and control strategies of the PI-Type-I fuzzy logic controller.

Figure 16 shows that the mathematical modelling of Type-III wind turbine system. In uses DFIG as the induction generator as it can use for both variable speed with modified full controller. In Fig. 17, it is the shot view of GSC of the grid where the Mode 4 Type-I fuzzy control with conventional PI controller is used to get faster response during transients to make the system more stable. As grid integration brings more transients and instabilities during speed variations this proposed technique can be help full to make the grid integrated wind energy system more stable.

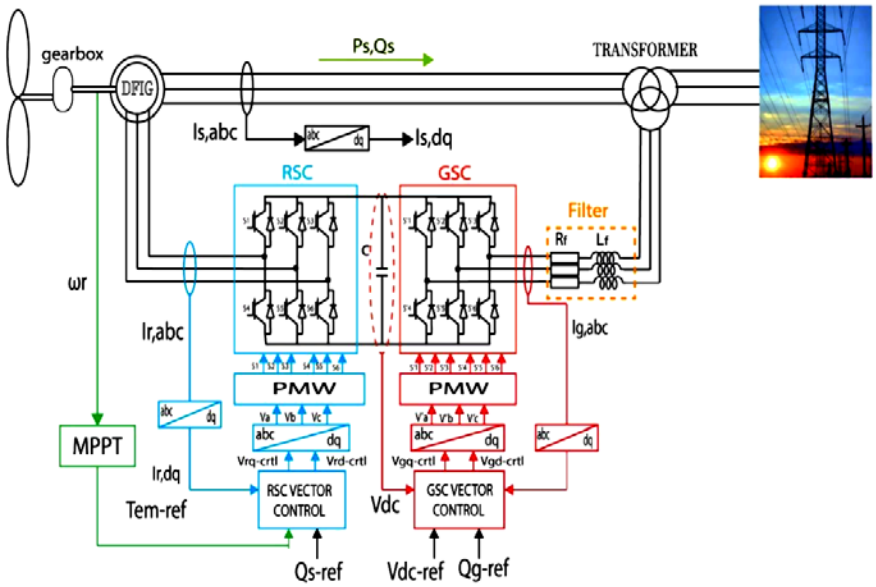

Fig.16. DFIG with WECS showing Type-III WT using controller.

Figure 18 shows the control action of series connected FACT devices with different wind speed variation on stator active power and reactive power. His result based on Fig. 15. Here both steady state and transient state analysis are done to know the better control action with exact settling time after fault clearance in a

single frame of graphical representations taking active and reactive power into consideration.

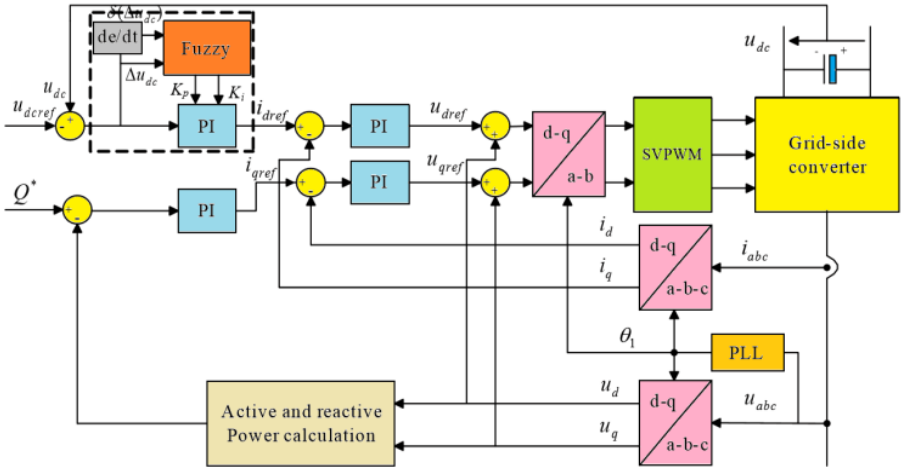

Fig.17. DFIG with WECS showing application of Type-I fuzzy logic controller.

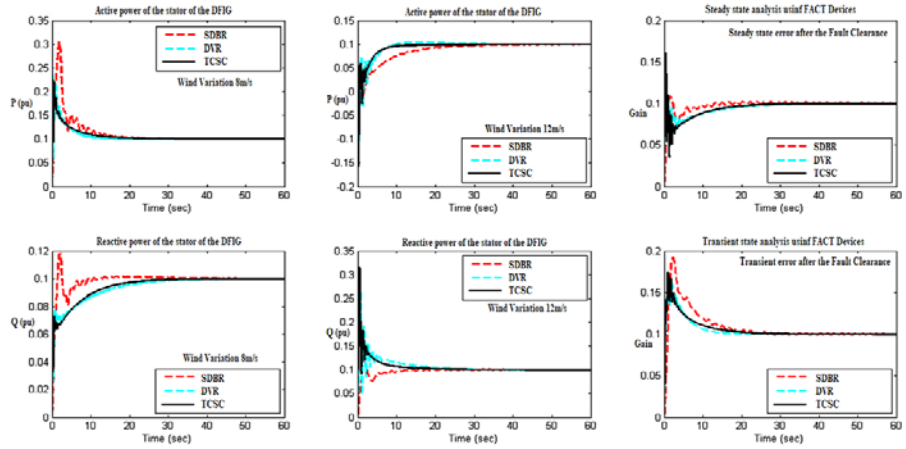

Fig.18. DFIG transient analysis using TCSC, DVR and SDBR (comparison).

Figure 19 illustrates that the variations of parameters with reference to (a) (without DVR), (b) (with DVR and PI) and (c) (DVR with Mode 4 Type-I FLC).

Below results are illustrating the proposed control (Mode 4 Type-I FLC) action of without using DVR and with DVR. Figure 20 shows the active power variations during different operating conditions and Fig. 21 illustrates the reactive power variations during the transients.

The numerical analysis of the Simulink results is shown in Table 1. The active power increased and reactive power decrease per unit to maintain the stability of the grid during faults. A phase and line faults (line to line and 3 phase faults) are taken for the transient study. The settling time is more in proposed technique clearly shown in Table 1.

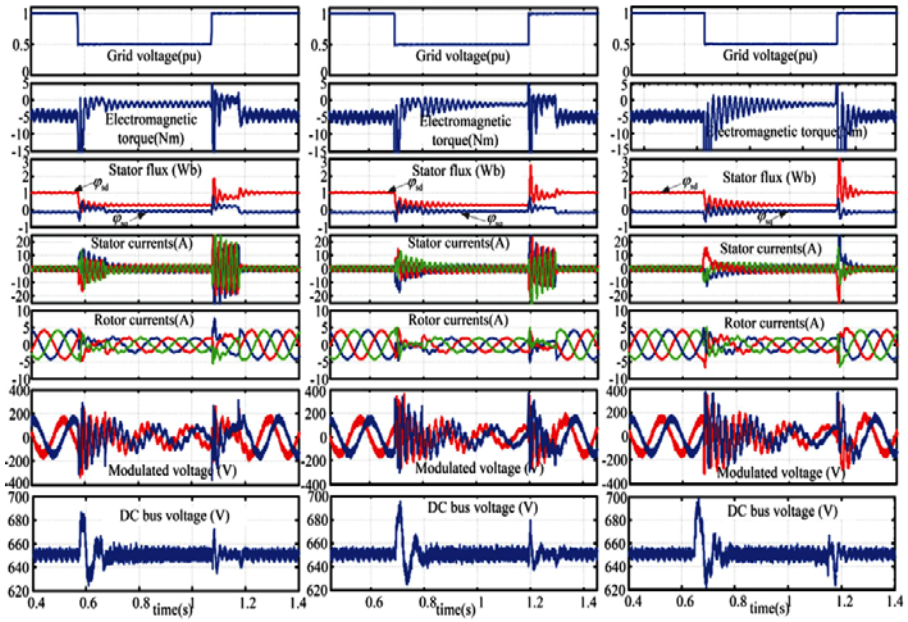

(a) (without DVR), (b) (with DVR and PI) (c) (DVR with Mode 4Type-I FLC).

Fig.19. DFIG transient analysis using DVR with control techniques.

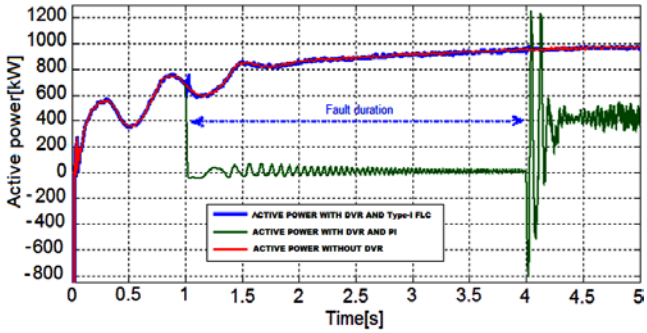

Fig.20. Active power control using DVR with control techniques.

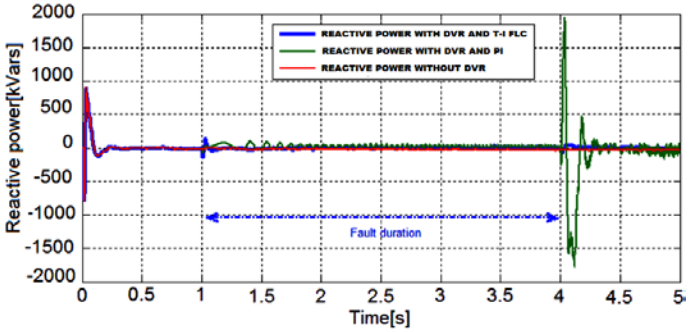

Fig.21. Reactive power control using DVR with control techniques.

From Table 1 shown below illustrates that the comparison between PI-FLC conventional Mode and PI-FLC proposed model. From Table 2 the total comparisons of all FACT devices are shown, and the performances are demonstrated. In Table 3 the parameters of the whole wind energy conversion system are shown and implemented in the Simulink.

Table 1. Comparison of DVR with proposed control technique.

Controller Parameters	**PI-FLC Type- I (Conventional)**	**PI-FLCType- I Mode** 4
Active Power	9.17 pu	9.8 pu
Reactive Power	9.50 pu	8.8 pu
Settling Time (3 Phase Fault)	0.1229sec	0.0777sec
Settling Time (Line Fault)	0.57212sec	0.5420sec

Table 2. Comparison of FACT devices.

Techniques/ Parameters	**SDBR**	**TCSC**	**DVR**	**MERS**	**FCL**
Complexity and wind speed measurement	Simple and required	Simple and not required	**Simple and required**	Simple and not required	Simple and not required
Speed of convergence	High	Low	**High**	High	Medium
Sensitivity	More	Less	**More**	More	Less
Tolerance to fast transitions	Medium	Low	**High**	High	High
Memory requirement	Recommend	Not required	**Not required**	Vary	Not required
Operational Knowledge	Recommend	Not required	**Recommend**	Recommend	Not required
Efficiency	**Medium**	**Low**	**Very Large**	**Large**	**Large**

Table 3. Parameters of wind energy conversion system model.

Parameters	**Value**
Wind Turbine Parameters	
Wind turbine rating	1.5 MW
Air density	1.225 kg/m^3
Rotor radius	30.66 m
Gear ratio	71.28
Wind cut-in speed	4 m/sec
Wind cut-out speed	25 m/sec
Rated wind speed	12 m/sec
Optimum TSR	5.7
Generator Parameters	
Capacity	1.5 MW
Voltage (L-L)	690 V
Frequency	60 Hz
Speed	2100 rpm
Reference Torque at t=0	-6631.45 Nm
Inertia constant	18.7 kg m^2
Control Parameters	

DC link voltage	1200 V
DC link capacitor	60 mF
Grid side Filter Parameters	
Filter resistance	0.002 ohm
Filter inductance	0.02

13. Analogy of Enhancement and Functional Approaches for WECS

Table 4 summarizes the effectiveness of the FACT devices.

Table 4. Series LVRT capability enhancement methods.

Methods		Conclusions	Limitation	Summary
FACT Devices	TCSC	• Capacitive reactance variations • Useful for fault current limitation and voltage unbalance	• High resonance • Heavy harmonic injection	• Offshore wind farm applicable • Per unit application is medium
	DVR	• Quick voltage recovery • Controlled reactive power	• Faster phase angle • Faster absorption of active power	• Compatible and high power usability • More stable
	SDBR	• Quick voltage recovery • Controlled reactive power	• No control on reactive power • High voltage damping • Poor low poor factor usage	• Per unit application is better • Less power system stability

Table 5 highlights the control action over faults during 8 m/s and 12 m/s wind speed variations. The Type-I fixed speed induction generator (FSIG) on using FACT devices gives voltage sag by 5% enhancements. This can be concluded that control action on wind turbine system FACT devices voltage sag by 0.06 sec and 0.8 sec.

Table 5. LVRT capability settling times (in sec).

Controller	Type I WT-TCSC	Type I WT-SDBR	Type I WT-DVR (Mode 4 Type-I FLC)
Wind Variation 8m/s	0.13	0.12	0.06
Wind variation 12m/s	0.16	0.15	0.08
Remark	Slow	Medium	Faster

Table 6 highlights the control action over faults during 8 m/s and 12 m/s wind speed variations. The Type-II variable speed induction generator without control action on using FACT devices gives voltage sag by 15% enhancements. This can be concluded that control action on wind turbine system FACT devices voltage sag of 0.7 sec and 0.8 sec pu sag condition.

Table 6. LVRT capability settling times (in sec).

Controller	Type II WT-TCSC	Type II WT-SDBR	Type II WT-DVR (Mode 4 Type-I FLC)
Wind Variation 8m/s	0.12	0.11	0.7
Wind variation 12m/s	0.15	0.14	0.8
Remark	Slow	Medium	Faster

Table 7 highlights the control action over faults during 8 m/s and 12 m/s wind speed variations.

Table 7. LVRT capability settling times (in m/sec).

Controller	Type III WT-TCSC	Type III WT-SDBR	Type III WT-DVR (Mode 4 Type-I FLC)
Wind Variation 8m/s	13.6	13.3	12.1
Wind variation 12m/s	15.7	14.1	13.9
Remark	Slow	Medium	Faster

The Type-III variable speed induction generator with control action on using FACT devices gives voltage sag by 25% to 35% enhancements. This can be concluded that control action on wind turbine system FACT devices voltage sag of 0.7 sec and 0.8 sec pu can be reduced by settling the fault by 12.1 millisecond and 13.9 millisecond for different wind speeds. In this research using Type-III wind turbine system it is conclude that the DVR is faster and better efficient as voltage enhancement during transients.

14. Conclusion

The activity of FACT devices and advancements for LVRT ability improvement of Type-III WTs using double fed induction generator presented in this research. The proposed controller Mode-4 Type-I fuzzy logic control technique associated with DVR gives more reliability to the grid during transients. At that point, all the control approaches of series connected arrangements are simulated and results are compared. It is concluded that rather than using conventional PI controller to DVR to control the grid profile, adaptive techniques can be implemented. Hence adaptive Type-I fuzzy logic controller is used to maintain the grid stabilities during transients. The dynamic and effective performance using different controllers the paper gives idea about complexity, cost economic and application reliabilities summarized in the comparison tabulations. Tables 5 and 6 summarize the proposed technique action on Type-I WT system (FSIG) and Type-II WT system, respectively. Table 7 illustrates the application of proposed control technique on Type-III WT. The simulations are generated using the programming software and the MATLAB/Simulink model. In this way, this operation on wind

energy system enables the analysts to comprehend the overall viability of the proposed auxiliary devices by controlling the active and reactive power during grid integrations. Due to rapid variation in wind speed this analysis in this research gives more impact to go for the proposed technique to maintain the stability of the system during transients.

Nomenclatures

Cp	Power coefficient
J	Moment of inertia, kg.m^2
P	Active power, W
Pwt	Wind power, kW
Q	Reactive power, kVAR
Te	Electromagnetic torque, N.m
Tm	Mechanical torque, N.m
Vw	Wind speed, m/s
$\vec{v}_s, \vec{v}_r$	Stator and rotor voltage, V
w_r^*	Reference rotor speed, rad/s
w_r	Actual rotor speed, rad/s

Greek Symbols

$\beta_{\_ref}$	Reference pitch angle, deg.
$\vec{\imath}_s, \vec{\imath}_r$	Stator and rotor current, A
λ	Tip speed ratio
$\vec{\lambda}_s, \vec{\lambda}_r$	Stator and rotor total flux linkage, Wb
ρ	Air density, kg/m^3
χ	Inductance, H

Abbreviations

DFIG	Double Fed Induction Generator
DVR	Dynamic Voltage Restorer
FLC	Fuzzy Logic Controller
GSC	Grid Side Controller
LVRT	Low Voltage Ride Through
PI	Proportional Integral
RPC	Reactive Power Compensation
RSC	Rotor Side Controller
SDBR	Series Dynamic Braking Resistor
TCSC	Thyristor Controlled Series Compensation
WECS	Wind Energy Conversion System

References

1. Moghadasi, A.; Sarwat, A.; and Guerrero, J.M. (2016). A comprehensive review of low-voltage-ride-through methods for fixed-speed wind power generators. *Renewable and Sustainable Energy Reviews*, 55, 823-839.
2. Ganthia, B.P.; and Barik, S.K. (2020). Steady-state and dynamic comparative analysis of PI and fuzzy logic controller in stator voltage oriented controlled

DFIG fed wind energy conversion system. *Journal of Institution of Engineers(India): Series B,*101, 273-286.

3. Ganthia, B.P.; Barik, S.K.; and Nayak, B. (2020). Shunt connected FACTS devices for LVRT capability enhancement in WECS. *Engineering, Technology and Applied Science Research,* 10(3), 5819-5823.
4. Ganthia, B.P.; Barik, S.K.; and Nayak, B. (2020). Application of hybrid facts devices in DFIG based wind energy system for LVRT capability enhancements. *Journal of Mechanics of Continua and Mathematical Sciences,* 15(6), 245-256.
5. Ganthia, B. P.; Barik, S. K.; and Nayak, B.; (2020). Transient analysis of grid integrated stator voltage oriented controlled type-III DFIGdriven wind turbine energy system. *Journal of Mechanics of Continua and Mathematical Sciences,* 15(6), 139-157.
6. Sun, L.; Peng, C.; Hu, J.; and Hou, Y. (2018). Application of type 3 wind turbines for system restoration. *IEEE Transactions on Power Systems*, 33(3),3040-3051.
7. Guest, E.; Jensen, K.H.; and Rasmussen, T.W. (2018). Sequence domain harmonic modeling of type-IV wind turbines. *IEEE Transactions on Power Electronics*, 33(6), 4934-4943.
8. Chen, X.; Yan, L.; Zhou, X.; and Sun, H. (2018). A novel DVR-ESS-embedded wind-energy conversion system. *IEEE Transactions on Sustainable Energy*, 9(3), 1265-1274.
9. Pragati, A.; Ganthia, B.P.; and Panigrahi, B.P. (2021). Genetic Algorithm Optimized Direct Torque Control of Mathematically Modeled Induction Motor Drive Using PI and Sliding Mode Controller. *Recent Advances in Power Electronics and Drives. Lecture Notes in Electrical Engineering*. vol 707. Springer, Singapore, 351-366
10. Muyeen, S.M.; Takahashi, R.; Murata, T.; and Tamura, J.A. (2010). A variable speed wind turbine control strategy to meet wind farm grid code requirements. *IEEE Transactions Power Syst*em, 25(1), 331-340.
11. Ganthia, B.P.; Pradhan, R.; Sahu, R.; and Pati, A.K. (2021). Artificial Ant Colony Optimized Direct Torque Control of Mathematically Modeled Induction Motor Drive Using PI and Sliding Mode Controller. *Recent Advances in Power Electronics and Drives. Lecture Notes in Electrical Engineering*. vol 707. Springer, Singapore. 389-408
12. Syed, M.H.; Zeineldin, H.H.; and Moursi, M.S. (2014). Hybrid micro-grid operation characterization based on stability and adherence to grid codes. *IET Generation, Transmission and Distribution,* 8(3), 563-572.
13. Ganthia, B.P.; Mohanty, S.; Rana, P.K.; and Sahu, P.K. (2016). Compensation of voltage sag using DVR with PI controller. *Proceedings of theInternational Conference on Electrical, Electronics, and Optimization Techniques*. Chennai, India, 2138-2142.
14. Ganthia, B.P.; Agarwal, V.; Rout, K.; and Pardhe, M.K. (2017). Optimal control study in DFIG based wind energy conversion system using PI & GA. *Proceedings of theInternational Conference on Power and Embedded Drive Control*. Chennai, India, 343-347.

15. Jerin, A.R.A.; Kaliannan, P.; Subramaniam, U.; and El Moursi, M.S.A. (2018). Review on FRT solutions for improving transient stability in DFIG-WTs. *IET Renewable Power Generation*, 12(15), 1786-1799.
16. Baloch, M.H.; Ishak, D.; Chaudary, S.T.; Ali, B.; Memon, A.A.; and Jumani, T.A. (2019). Wind power integration: an experimental investigation for powering local communities. *Energies*, 12(4), 1-24.
17. Saeed, M.A.; Khan, H.M.; Ashraf, A.; and Qureshi, S.A. (2018). Analyzing effectiveness of LVRT techniques for DFIG wind turbine system and implementation of hybrid combination with control schemes. *Renewable and Sustainable Energy Reviews*, 81(2), 2487-2501.
18. Niu, L.; Wang, X.; Wu, L.; Yan, F.; and Xu, M.(2019). Review of low voltage ride-through technology of doubly-fed induction generator. *The Journal of Engineering*, 2019(16), 3106-3108.
19. Din, Z.; Zhang, J.; Zhu, Y.; Xu, Z.; and El-Naggar, A.(2019). Impact of grid impedance on LVRT performance of DFIG system with rotor crowbar technology. *IEEE Access*, 7, 127999-128008.
20. Naderi, S.B.; Negnevitsky, M.; and Muttaqi, K.M. (2019). A modified DC chopper for limiting the fault current and controlling the DC-link voltage to enhance fault ride-through capability of doubly-fed induction-generator-based wind turbine. *IEEE Transactions on Industry Applications*, 55(2), 2021-2032.